Available online at www.sciencedirect.com

ScienceDirect

Ceramics International 41 (2015) 743–748

CERAMICS INTERNATIONAL

www.elsevier.com/locate/ceramint

Synthesis and characterization of $Y_2O_3:Pr^{3+}$ phosphor powders by simple solvent evaporation

G. Alarcón-Flores[a,*], M. García-Hipolito[b], M. Aguilar-Frutis[a], E. Zaleta-Alejandre[c], Cecilia Chacón[a], F. Ramos-Brito[d], S. Carmona-Téllez[e], J. Guzmán-Mendoza[a], C. Falcony[c]

[a]Centro de Investigación en Ciencia Aplicada y Tecnología Avanzada—Legaría del Instituto Politécnico Nacional, Legaría 694, Colonia Irrigación, CP 11500, México, D.F., Mexico

[b]Instituto de Investigaciones en Materiales, Universidad Nacional Autónoma de México, Apdo. Postal 70-360, Del. Coyoacán, CP 04150, México, D.F., Mexico

[c]Universidad Autónoma del Estado de Hidalgo—Escuela superior de Apan, Carretera Apan—Calpulalpan, Km 8, CP 43920, Apan, Hidalgo, México, Mexico

[d]Laboratorio de Materiales Optoelectrónicos, DiDe, Centro de Ciencias de Sinaloa, Av. De las Américas No 2771 Nte, Col. Villa Universidad, CP 80010, Culiacán, Sinaloa, Mexico

[e]Instituto de Física, Universidad Nacional Autónoma de México, Del. Coyoacán, CP 04150, México, D.F., Mexico

Received 29 July 2014; received in revised form 28 August 2014; accepted 29 August 2014
Available online 6 September 2014

Abstract

The synthesis of trivalent praseodymium doped yttrium oxide powders ($Y_2O_3:Pr^{3+}$) by the solvent evaporation method as well as their structural and luminescent (cathodoluminescence and photoluminescence) properties are reported as a function of the concentration of the reagents and annealing temperatures in the 400 to 1100 °C range. These powders become polycrystalline in a cubic Y_2O_3 structure at temperatures above 600 °C. An increase in the diffraction peaks intensity was observed as the temperature is increased. Transmission electron microscopy analysis showed irregular needle like crystallites and the characteristic electron diffraction rings for polycrystalline powders on samples annealing above 600 °C. Scanning electron microscopy showed that these crystallites clump into larger particles of irregular shape. Luminescence spectra show the characteristic peaks at 620 and 630 nm due to $^1D_2$ to $^3H_4$ transitions in Pr^{3+} ions in the Y_2O_3 host.

Keywords: Polycrystalline powders; Yttrium oxide; Trivalent praseodymium; Photoluminescence spectroscopy

1. Introduction

Yttrium oxide has been considered an interesting material for various scientific and technological applications because its physical and chemical properties such as a high dielectric constant (13–18), [1–3] a high refractive index (~2), good thermal expansion coefficient and high thermal conductivity. It also possess large energy bangap (~6 eV) [4] and high mechanical strength [5]. The wide band-gap is quite appropriated for its use as host material for lanthanide elements on light-emitting devices applications [6–8]. Its cubic crystalline form has 8 (C_{3i}) and 24 (C_2) Y sites, which have a high probability of being occupied by lanthanide ions [3]. It also presents a relatively low phonon energy (430–550 cm^{-1}), which can increase the probability of radiative electronic transitions [9,10]. Pr^{3+} doped materials are of great interest, because (Pr^{3+}) trivalent ion has an energy level scheme containing several multiplets resulting in different emissions lines in the visible, although the most intense emission is red light from a $^1D_2$ to $^3H_4$ transition. An additional advantage of Pr^{3+} doped materials is that its luminescence emission can be excited with blue light easily obtainable from GaN diodes (LED, LD) which are commercially available at low cost. Therefore, these materials could be used as luminescent materials for white light emitting diodes, scintillators and 3D visual displays [11–13]. The synthesis of this phosphor by low cost wet based methods includes sol–gel [14,15], urea precipitation [16] and co-precipitation [17,18]. These methods involve multiple steps including: reagents

*Corresponding author.

http://dx.doi.org/10.1016/j.ceramint.2014.08.133
0272-8842/

dissolution sometimes with heating, and longer reaction time with heating (several hours). In general, the powder obtained is amorphous and requires centrifugation washing, drying and high temperature annealing for crystallization. The crystallite size depends on the annealing temperature (up to 1300 °C) and it is usually larger for higher temperatures [18,19].

In this work, the structural and luminescent characteristics of praseodymium doped yttrium oxide powders by the solvent evaporation method are reported. This method is characterized by its simplicity, low cost, and short sample preparation times. The characterization of these powders was performed as a function of the activator ion concentration and annealing temperatures. High luminescent (photo- and cathodoluminescence) emission intensity was obtained due to intra electronic energy levels transitions $^1D_2$ to $^3H_4$ and $^1D_2$ to $^3H_5$ of the Pr^{3+} ions in the Y_2O_3 host lattice.

2. Experimental procedure

The synthesis of Y_2O_3:Pr^{3+} powders by the solvent evaporation method involved the preparation of mixtures obtained by dissolving $Y(NO_3)_3$ and $PrCl_3$ in methanol, varying the atomic percent (at%) of Pr [0.04, 0.07, 0.15 and 0.30] in relation to the Y content in the starting mixture. These mixtures were heated at 60 °C for 90 min in an oxidizing atmosphere (air) until the solvent was completely evaporated. The obtained powders were annealed in alumina crucibles at different temperatures, 400 to 1100 °C for 3 h. A Siemens D-5000 XRD system with CuK_α (λ=1.5406 Å) was used to determine the crystal structure. The crystal size was estimated by the Scherrer's formula (Eq. (1)) [20].

$$T = \frac{0.9\lambda}{B \cos \theta_B} \quad (1)$$

where: T represents crystallite size, λ the wavelength of CuK_α radiation, B the half width of the diffraction peak and θ_B the Bragg's angle in radians.

Transmission electron microscope (TEM) images were performed using a JEOL 2010 microscope. The surface morphology of the powders was observed by using a scanning electron microscope (SEM) with an accelerating voltage of 10 kV. The luminescence measurements were obtained from the powders pressed into pellets (1.3 cm in diameter and ~1.5 mm thick). A SPEX Fluoro-Max-P spectrofluorometer was used for photoluminescence measurements and a Luminoscope, model ELM-2 MCA, by RELION Co. was used for cathodoluminescence measurements. In this case the diameter of the electron beam on the pellet was approximately 3 mm and the emitted light was collected by an optical fiber and fed into the spectrofluorometer mentioned above. The applied current of electron beam was 0.1 mA with an accelerating voltage in the range from 2 to 7 kV. All luminescence measurements were performed at room temperature.

3. Results and discussion

Fig. 1 shows XRD measurements for 0.15 at% Pr^{3+} doped Y_2O_3 powders annealed at different temperatures. The films

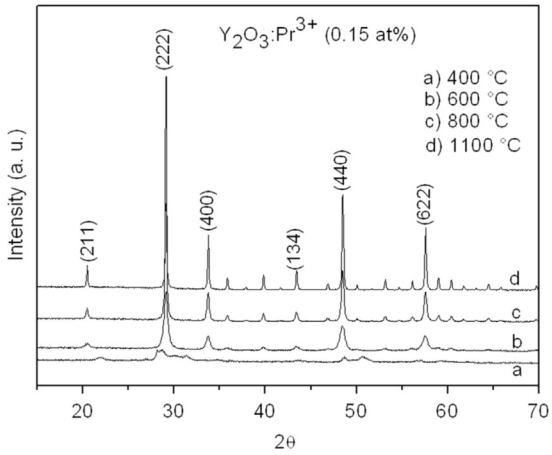

Fig. 1. X-ray diffractograms of the Y_2O_3:Pr^{3+} powders at different annealing temperatures. The $PrCl_3$ concentration in the start mixture was 0.15 at%.

were polycrystalline with a cubic Y_2O_3 crystalline structure. The diffraction peaks increased with increasing annealing temperature indicating that the crystalline structure of the powder was improving. The peaks, located at 2θ=29.1°, 32.9°, 48.5° and 57.6°, are associated with the (2 2 2), (4 0 0), (4 4 0) and (6 2 2) directions, respectively. These lines correspond to the Y_2O_3 cubic phase according to the JCPDS 43-1036 diffraction card; with a lattice parameter of 10.604 Å. Average particle size was estimated with the Scherrer formula to be about 15 nm, for the samples annealed at 600 °C and 35 nm for the sample annealed at 1100 °C. Therefore, it is evident that the Pr^{3+} doped Y_2O_3 powders contain only cubic crystalline phase with an *Ia*3 space group, where Y^{3+} and Pr^{3+} ions are placed at 32 sites in the unit cell, 24 sites with point group symmetry C_2 and 8 sites with C_{3i} symmetry [21]. It is observed that there are not significant differences between the un-doped and the Pr^{3+} doped Y_2O_3 samples XRD patterns, probably because the amount of praseodymium added was low. The chemical similarities between yttrium and praseodymium ions permit the substitution of Y^{3+} ions with Pr^{3+} ions into the Y_2O_3 crystalline structure. Y^{3+} and Pr^{3+} have ionic radius of 104 and 113 pm respectively, therefore it is not surprising that no major crystalline differences are observed between doped and un-doped powders.

To corroborate the polycrystalline nature of the powders, these were studied by SEM and TEM. Fig. 2 shows the micrographs representative of Y_2O_3:Pr^{3+} (0.15 at% Pr^{+3}) annealed powders at 600 and 1100 °C for 3 h. The image for the sample annealed at 800 °C is not included because it is similar to those obtained at 600 °C. Fig. 2a and d correspond to images SEM of annealed powders at 600 and 1100 °C respectively. These images revealed aggregated microstructures of irregular shape with a tendency to get needle-like crystals. In the TEM images (Fig. 2b and e), it can be observed that the powder obtained at 600 °C show needle-like crystals of nanometer size and in the sample annealed at 1100 °C it was revealed rod-like crystal of a larger size. This behavior can be confirmed from selected-area electron diffraction (SAED) pattern recorded perpendicularly to the needle-like crystals which showed concentric rings indicating the presence of the small crystal

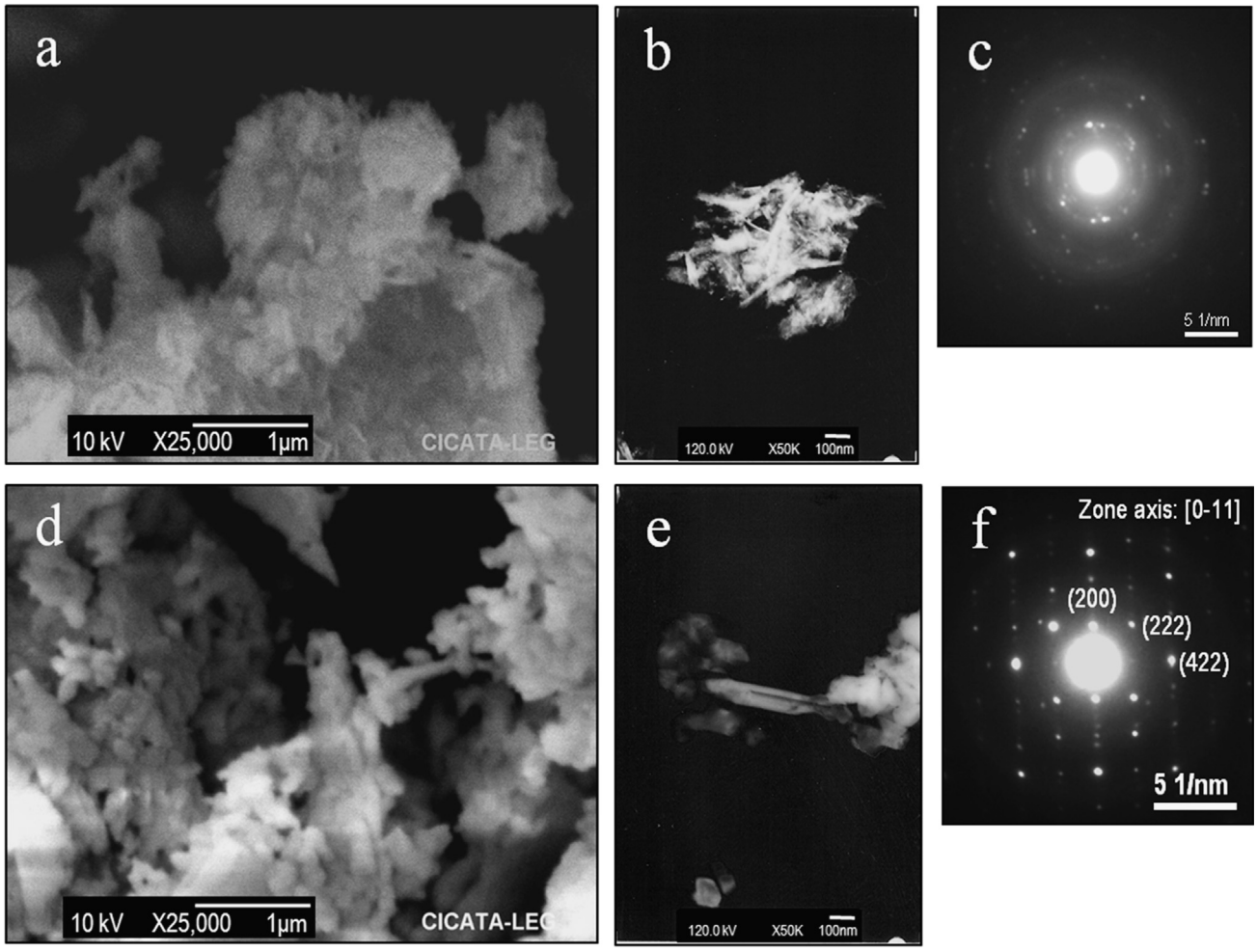

Fig. 2. (a) and (d) SEM images Y_2O_3:Pr^{3+} (0.15 at%) powders annealed at 600 and 1100 °C for 3 h, ((b) and (e)) representative TEM images Y_2O_3:Pr^{3+} (0.15 at%) powders calcined at 600 and 1100 °C and ((c) and (f)) correspond to SAED patterns of powders at 600 and 1100 °C.

(see Fig. 2c). In contrast, the SAED pattern of rod-like crystal (Fig. 2f) showed highly crystalline structure, which can be inferred by the well-defined electron diffraction pattern that confirms the presence of (2 0 0), (2 2 2) and (4 2 2) planes of cubic Y_2O_3. The common zone axis to the observation field is the direction (0 1 1). Previous results indicate that when Y_2O_3:Pr^{3+} powder was annealed at 600 °C the poor crystalline leads in small crystal size. When the annealing temperatures are up to 1100 °C, the crystal size increases and the particles have a regular shape. The increase average crystallite size is directly related to the increase of the crystals quality of the Y_2O_3:Pr^{3+} powders as a function of the annealing temperature. The indexing of the diffraction patterns corresponds to the Y_2O_3 cubic phase in agreement with the XRD results described above (JCPDS card No 43-1036).

The photoluminescence excitation spectrum for the 0.15 at% Pr^{3+} doped Y_2O_3 annealed at 1100 °C at the emission wavelength of 620 nm is plotted in Fig. 3. This spectrum shows the peaks at 458, 472, 485 and 497 nm, associated with the excitation transitions $^3P_2$, $^1I_6$, $^3P_1$, and $^3P_0$, respectively. The peak centered at ~288 nm (the most intense) is probably associated with charge transfer (CT) from Pr^{3+}–O localized states in the Y_2O_3 lattice, as in the case of Eu–O CT reported for the same host [11].

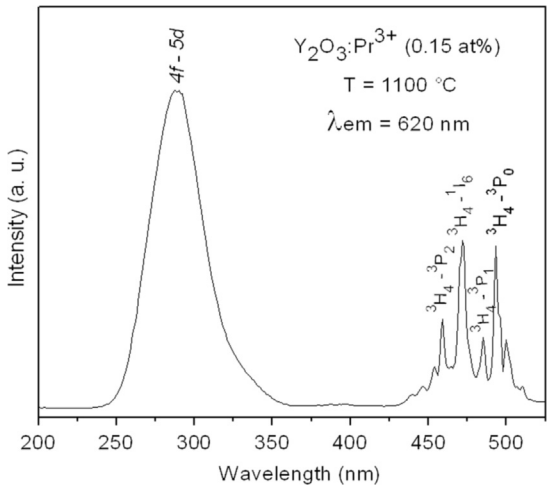

Fig. 3. Excitation spectrum obtained for Y_2O_3:Pr^{3+} powder with 0.15 at% of $PrCl_3$ in the start mixture and with an annealing temperature of 1100 °C. The emission wavelength fixed at 620 nm.

Fig. 4 shows the photoluminescence emission spectra for samples annealed at 1100 °C with different dopant concentrations and excitation wavelength of 288 nm. These emission

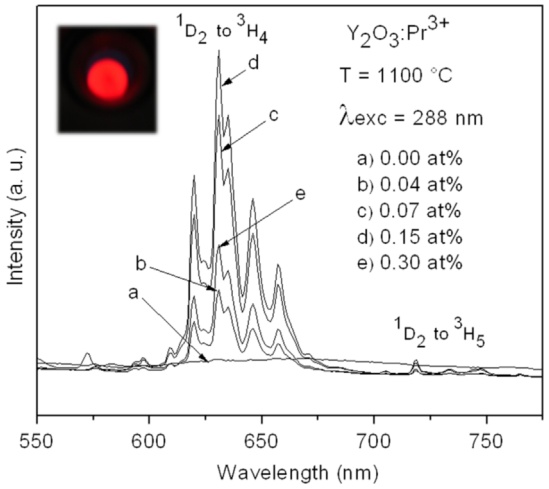

Fig. 4. Behavior of PL emission spectra as a function of doping concentration for $Y_2O_3:Pr^{3+}$ powders. The annealing temperature was 1100 °C and the excitation wavelength was fixed at 288 nm. (For interpretation of the references to color in this figure legend, the reader is referred to the web version of this article.)

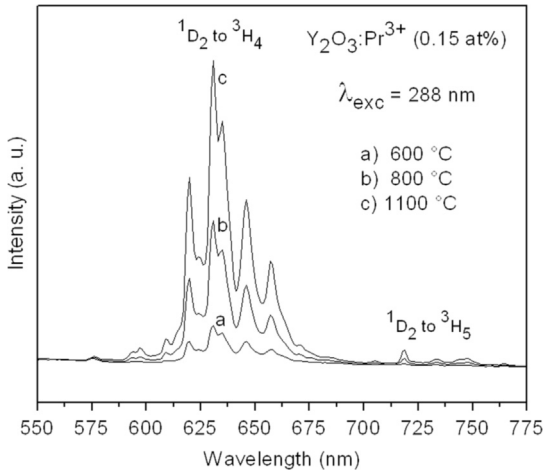

Fig. 5. Behavior of PL emission spectra as a function of the annealing temperature for $Y_2O_3:Pr^{3+}$ powders. The $PrCl_3$ concentration in the start mixture was 0.15 at% and the excitation wavelength was 288 nm.

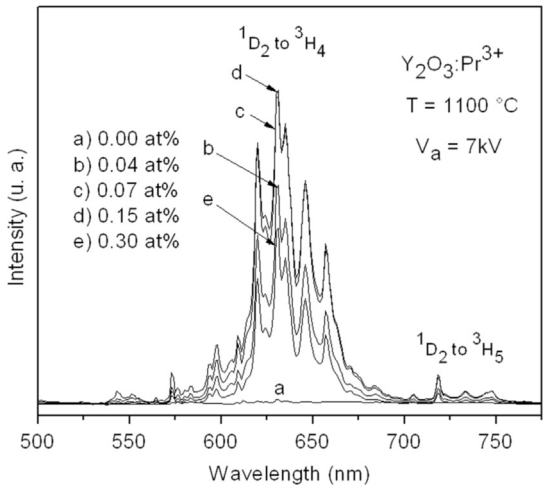

Fig. 6. Behavior of CL emission spectra as a function of doping concentration for $Y_2O_3:Pr^{3+}$ powders. The annealing temperature was 1100 °C and the electron accelerating voltage was 7 kV.

spectra present peaks in the 565 to 690 nm and 700 to 775 nm ranges, characteristic for Pr^{3+} intra-electronic energy levels transitions in particular from the $^1D_2$ excited state to the $^3H_4$ and $^3H_5$ ground states, respectively [6,10,14–16]. The PL emission intensity increases with the doping concentration up to a maximum emission intensity at 0.15 at% of $PrCl_3$ in the starting mixture. A concentration quenching is observed for higher dopant concentrations. The electronic transitions from $^1D_2$ excited state to $^3H_{J's}$, ground state are associated with large phase shift for $4f^15d^1$ excited band with respect to $4f^2$ ground states in a configuration coordinate diagram. This allows that the $4f^15d^1$ states cross the $^3P_{J's}$ and $^1D_2$ states, so that the $^3P_{J's}$ state relaxes non-radiatively to the $^1D_2$ state, via the lying $4f^15d^1$ band [22]. Multiphonon emission from ^3P_J levels to $^1D_2$ levels is not produced due to the low phonon energy of $\omega_{max}=550\ cm^{-1}$ in the lanthanides oxides with cubic structure. Also it can be observed that the relative intensity of the transition $^1D_2$ to $^3H_5$ is smaller than $^1D_2$ to $^3H_4$ [23–25]. The inset in Fig. 4 shows a photograph of a sample under UV excitation at 253 nm, in which an intense red–orange emission is observed.

Fig. 5 shows the PL emission spectra of 0.15 at% Pr^{3+} doped Y_2O_3 as a function of the annealing temperatures. Here it can be observed that the PL emission intensity increases as the annealing temperature is raised. This may be attributed to the fact that as the temperature is increased a better and larger crystallites are generated in the host material, therefore a better arrangement of the Pr^{3+} ions on crystallographic sites (C_2/Y (24d) and C_{3i}/S_6Y(8b)) into the Y_2O_3 cubic lattice is achieved [11]. This is also supported by the XRD and TEM results [13]. In Figs. 4 and 5 it can be seen that the PL emission spectra structure does not change when the doping concentration and temperature varies, although there is a change in the emission intensity. In the same way, it can also be observed that the relative intensity of $^1D_2$ to $^3H_5$ transition to respect $^1D_2$ to $^3H_4$ transition does not change. Above mentioned suggests that the surroundings in which the Pr^{3+} ion is immersed is independent of the doping concentration and temperature, at least, for the values here studied.

Fig. 6 shows the cathodoluminescent emission spectra for the Pr^{3+} doped Y_2O_3 powders sintered at 1100 °C for different doping concentration in the spraying mixture for an electron accelerating potential of 7 kV. The behavior of these spectra is similar to the one observed for the PL spectra. The only difference between these two spectra is that the intensity at the main peak with 0.07 at% is the same as that for 0.15 at%, as can be seen in this figure. The difference with respect to the PL spectra for both concentrations is probably due to the difference in excitation mechanisms. Cathodoluminescent emission intensity is, in general, higher than photoluminescent emission intensity for $^1D_2$ to $^3H_4$ and $^1D_2$ to $^3H_5$ electron transitions.

Fig. 7 shows the cathodoluminescent emission spectra of the $Y_2O_3:Pr^{3+}$ powders for different annealing temperatures for

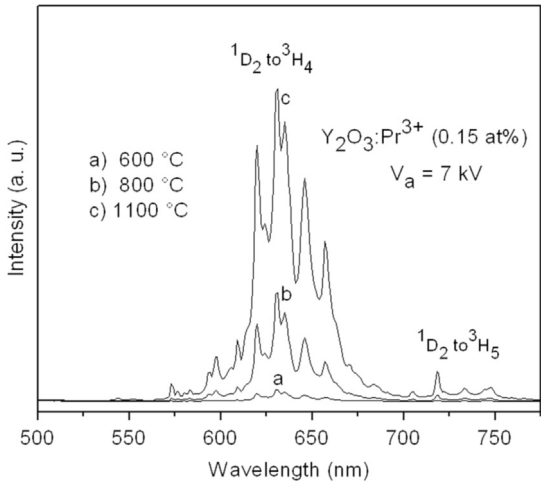

Fig. 7. Behavior of CL emission spectra as a function of the annealing temperature for Y_2O_3:Pr^{3+} powders. The $PrCl_3$ concentration in the start mixture was 0.15 at% and the electron accelerating voltage was 7 kV.

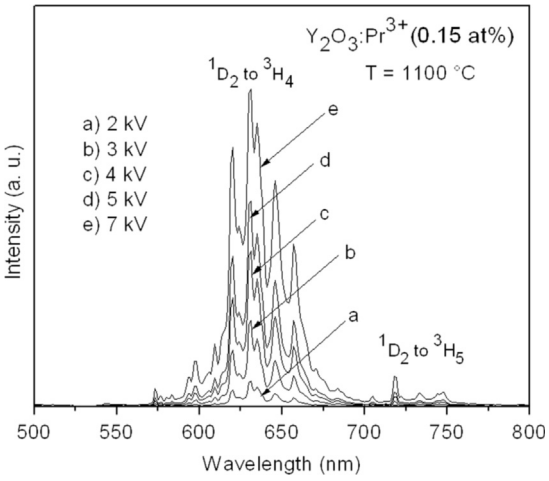

Fig. 8. Behavior of CL emission spectra as a function of electron acceleration voltage for Y_2O_3:Pr^{3+} powders. The $PrCl_3$ concentration in the star mixture was 0.15 at% and the annealing temperature was 1100 °C.

0.15 at% dopant concentration powders and an electron beam accelerating voltage of 7 kV. The behavior is similar to that observed in PL (Fig. 5), i.e. the CL emission intensity increases as the annealing temperature is increased. The most intense PL emission was obtained at 1100 °C.

Fig. 8 shows cathodoluminescent emission intensity of Y_2O_3:Pr^{3+} as a function wavelength for different electron acceleration voltages, it is noted that the emission intensity is proportional to the electrons accelerating voltage. This can be attributed to the larger penetration of the electron beam into the analyzed material as the acceleration voltage is increased, since a larger volume of material is excited in this way.

4. Conclusion

Luminescent polycrystalline Pr^{3+} doped Y_2O_3 powder was obtained by the solvent evaporation method followed by an annealing process at different temperatures above 400 °C. These powders presented the Y_2O_3 cubic polycrystalline structure and the crystallite size was in the 15 to 35 Å range, the largest corresponding to the highest annealing temperature of 1100 °C. The luminescence intensity was also proportional to the annealing temperature and presented the characteristic red–orange emission associated with the intra-electronic energy level transitions of the Pr^{3+} ion. Both cathodoluminescence and photoluminescence presented maximum emission intensity at 0.15 at% Pr^{3+} concentration and a quenching effect for larger concentration values is observed.

Acknowledgements

The authors acknowledge the financial support of DGAPA-UNAM and SIP-IPN through research projects: 20130236, 20130153, 20140458, and 20140459.

References

[1] J.J. Araiza, M.A. Aguilar-Frutis, C. Falcony, Optical, electrical, and structural characteristics of yttrium oxide films deposited on plasma etched silicon substrates, J. Vac. Sci. Technol. B 19 (2001) 2206.
[2] G. Alarcón-Flores, M. Aguilar-Frutis, C. Falcony, M. García-Hipolito, J.J. Araiza-Ibarra, H.J. Herrera-Suárez, Low interface states and high dielectric constant Y_2O_3 films on Si substrates, J. Vac. Sci. Technol. B 24 (2006) 1873.
[3] Y. Guyot, R. Moncorge, L.D. Merkle, A. Pinto, B. McIntosh, H. Verdum, Luminescence properties of Y_2O_3 single crystals doped with Pr^{3+} or Tm^{3+} and codoped with Yb^{3+}, Tb^{3+} or Ho^{3+} ions, Opt. Mater. 5 (1996) 127.
[4] J. Robertson, High dielectric constant gate oxides for metal oxide Si transistors, Rep. Prog. Phys 69 (2006) 327.
[5] R.J. Gaboriaud, Fluage haute temperature du sesquioxyde d'yttrium: Y_2O_3, Philos. Mag. A 44 (1981) 561.
[6] J.C. Alonso, E. Haro-Poniatoswski, R. Diamant, M. Frenández-Guasti, M. García, Photoluminescent thin films of terbium chloride-doped yttrium oxide deposited by the pulsed laser ablation technique, Thin Solid Films 303 (1997) 76.
[7] M. García-Hipólito, O. Alvarez-Fregoso, E. Martinez, C. Falcony, M.A. Aguilar-Frutis, Characterization of ZrO_2:Mn, Cl luminescent coatings synthesized by the Pyrosol technique, Opt. Mater., 20, , 2002, p. 113.
[8] J.H. Mun, A. Jouini, A. Novoselov, Y. Guyot, A. Yoshikawa, H. Ohta, H. Shibata, Y. Waseda, G. Boulon, T. Fukuda, Growth and characterization of Tm-doped Y_2O_3 single crystals, Opt. Mater. 29 (2007) 1390.
[9] G.C. Aumüller, H. Boysen, F. Frey, B.C. Grabmaier, Defects in insulating materials, in: Proceedings of the 12th International Conference, World Scientific Publishing Co. Inc., (1993), pp. 1211.
[10] Shiwei Wang Jian Zhang, Tianjun Rong, Lidong Chen, Upconversion luminescence in Er^{3+} doped and Yb^{3+}/Er^{3+} codoped yttria nanocrystalline powders, J. Am. Ceram. Soc. 87 (2004) 1072.
[11] G. Blasse, B. Grabmaier, Luminescent Materials, Springer-Verlag, 1994, p. 45.
[12] F. Ramos Brito, M. García Hipólito, C. Alejo Armenta, O. Alvarez Fragoso, C. Falcony, Characterization of luminescent praseodymium-doped ZrO_2 coatings deposited by ultrasonic spray pyrolysis technique, J. Phys. D: Appl. Phys 40 (2007) 6718.
[13] M. Dudek, A. Jusza, K. Anders, L. Lipińska, M. Baran, R Piramidowicz, Luminescent properties of praseodymium doped Y_2O_3 and $LaAlO_3$ nanocrystallites and polymer composites, J. Rare Earths 29 (2011) 1123.
[14] Stéphane Daniele, Liliane G. Hubert-Pfalzgraf, Synthesis of nanocrystalline Y_2O_3/Pr^{3+} from heterometallic alkoxide via sol–gel process, Mater. Lett. 58 (2004) (1989).

[15] H. Guo, W. Zhang, L. Lou, A. Brioude, J. Mugnier, Structure and optical properties of rare earth doped Y_2O_3 waveguide films derived by sol–gel process, Thin Solid Films 458 (2004) 274.

[16] Y. Sun, L. Qi, M. Lee, B.I. Lee, W.D. Samuels, G.J. Exarhos, Photoluminescent properties of Y_2O_3:Eu^{3+} phosphors prepared via urea precipitation in non-aqueous solution, J. Lumin., 109, , 2004, p. 85.

[17] P. Maestro, D. Huguenin, A. Seigneurin, F. Deneuve, P. Le Lann, J.F Berar, Mixed rare earth oxides as starting material for the preparation of Y_2O_3:Eu lamp phosphor: characterization and use, J. Electrochem. Soc. 139 (1992) 1479.

[18] S Erdei, R. Roy, G. Harshe, H. Juwhari, D. Agraeal, F.W. Ainger, W.B. White, The effect of powder preparation processes on the luminescent properties of yitrium oxide based phosphor materials, Mater. Res. Bull. 30 (1995) 745.

[19] T. Hase, T. Kano, E. Nakasawa, H. Yamamoto, Adv. Electron. Electron. Phys. 79 (1990) 325.

[20] B.D. Cullit, S.R. Stock, Elements of X-Ray Diffraction, Prentice-Hall Inc., 2001, p. 388.

[21] John A. Capobianco, Fiorenzo Vetrone, J. Christopher Boyer, Adolfo Speghini, Marco Bettinelli, Enhancement of red emission ($^4F_{9/2}$ to $^4I_{15/2}$) via upconversion in bulk and nanocrystalline cubic Y_2O_3:Er^{3+}, J. Phys. Chem. B 106 (2002) 1181.

[22] G.C. Aumüller, W. Kloster, B.C. Grabmaier, R. Frey, Luminescence properties of Pr^{3+} in cubic rare earth oxides, J. Phys. Chem. Solids 55 (1994) 767.

[23] B. Savoini, J.E. Muños Santiuste, R González, Optical characterization of Pr^{3+} doped yttria-stabilized zirconia single crystals, Phys. Rev. B: Condens. Matter 56 (1997) 5856.

[24] Ho Seong Jang, Won Bin Im, Dong Chin Lee, Duk Young Jeon, Shi Surk Kim, Enhancement of red spectral emission intensity of $Y_3Al_5O_{12}$:Ce^{3+} phosphor via Pr co-doping and Tb substitution for the application to white LEDs, J. Lumin. 126 (2007) 371.

[25] E.W. Chase, R.T. Hepplewhite, D.C. Krupka, D. Kahng, Electroluminescence of ZnS lumocen devices containing rare-earth and transition-metal fluorides, J. Appl. Phys. 40 (1969) 2512.